Coulostatic Potential Transients Induced by Laser Heating of a Pt(111) Single-Crystal Electrode in Aqueous Acid Solutions. Rate of Hydrogen Adsorption and Potential of Maximum Entropy

Víctor Climent, Barry A. Coles, and Richard G. Compton*

Physical and Theoretical Chemistry Laboratory, Oxford University, South Parks Road, Oxford OX1 3QZ, United Kingdom

Received: March 21, 2002

Short pulses (∼10 ns) of high-power laser light produce a sudden increase in the surface temperature of a Pt(111) single-crystal electrode in acidified potassium perchlorate or sulfate solutions. The change of the electrode potential at open circuit was monitored during the relaxation of the temperature. At low pH, the potential transients in the hydrogen adsorption region exhibit a bipolar shape, which can be explained considering that the relaxation is influenced by the rate of hydrogen adsorption. With this assumption, we have estimated a value of the rate constant for hydrogen adsorption around 8×10^6 M^{-1} s^{-1}. By increasing the pH, the rate of hydrogen adsorption is reduced, making it possible to decouple the double-layer response from the hydrogen adsorption process. In this case, the potential where the double-layer response to the temperature increase is zero can be identified with the potential of maximum entropy of formation of the double layer. This potential is located in the double-layer region (ca. 0.43 V vs Pd/H_2) for a solution of pH 3. The relevance of this measurement in terms of the location of the potential of zero charge is discussed.

1. Introduction

We have previously used laser illumination to increase an electrode temperature over a very short time scale. From the analysis of the electrochemical response, either the current in potentiostatic mode[1] or the potential in coulostatic mode,[2] it has been possible to obtain information about the electrochemical double layer in contact with a Au(111) single-crystal electrode. With this approach, two key characteristics of the electrochemical double layer can be obtained, namely, the potential of zero charge (pzc)[1] and the potential of maximum entropy (pme).[2] Moreover, we have shown that the pme is located at potentials slightly negative with respect to pzc. This result is consistent with independent observations on both solid electrodes[3−5] and mercury[6−8] and it is explained in the framework of models of the double layer as a consequence of the natural orientation of the water dipoles at the pzc with the negative end toward the metallic surface.[9]

Since the introduction of the flame-annealing technique by Clavilier[10,11] a great amount of information has been obtained about the electrochemical behavior of platinum single crystals. In particular, the important role played by the superficial structure on both kinetic and thermodynamic aspects has been often emphasized. However, our knowledge of the structure of the double layer is far from complete and several aspects remain controversial. One aspect that has been revisited several times in the past decade has been the pzc of platinum single-crystal electrodes.[12−19] This subject is complicated by the existence of hydrogen and anion adsorption processes on platinum electrodes that involve charge transfer. Hence, the interface cannot be considered strictly as ideally polarizable (although the interface can be polarized without getting a stationary faradaic current) and the microscopic distribution of charges in the interphase cannot be deduced by only thermodynamic means. In this case, the proper notion of the electrode charge needs to distinguish between the total charge, which includes the charge involved in the adsorption processes, and the free charge, which is the actual charge residing on the metallic side of the electrochemical double layer.

In the present work we apply the coulostatic temperature jump experiment to get information about the Pt(111)/acidic electrolyte interface. This system is particularly suitable for analysis, since the hydrogen and anion adsorption processes, which overlap in electrodes with other crystallographic orientations, are well separated.

Little work exists on the study of the kinetics of the hydrogen underpotential deposition on platinum single-crystal electrodes. This study is complicated by the very fast nature of this process. In particular the rate of hydrogen adsorption on Pt(111) has eluded measurement, and the process behaves as "reversible" even with modulation of the potential as fast as 100 kHz.[20] To our knowledge, only very recently have impedance measurements been extended to the megahertz frequency range and become able to decouple the adsorption process from the double-layer capacitance.[21]

We show below that potential transients in the hydrogen adsorption region induced by the laser heating of the Pt(111) electrode can be understood using a simple model for the kinetic of hydrogen adsorption according to a Frumkin adsorption isotherm. With this model it is possible to show that the potential transients will be affected by the kinetics of hydrogen adsorption only over a certain range of rate constants. For slower processes, hydrogen adsorption cannot follow the very fast change of the interfacial temperature, and the potential change will reflect only the response of the double layer to the temperature change. On the other hand, if the kinetics are fast enough, the equilibrium

* To whom all correspondence should be addressed. E-mail: compton@ermine.ox.ac.uk,. Tel.: +44 (0) 1865 275 413. Fax: +44 (0) 1865 275 410.

10.1021/jp020785q CCC: $22.00
Published on Web 05/21/2002

will follow the temperature change and only thermodynamic information of the equilibrium can be obtained. The experimental potential transients exhibit the behavior expected for the intermediate case in which the kinetics of the adsorption process affects the response. This makes possible the estimation of a rate constant value for the hydrogen adsorption process.

On the other hand, decreasing the concentration of protons can reduce the rate of hydrogen adsorption, decoupling it from the response of the double layer. By doing this, a potential of zero response of the double layer can be measured and identified with the pme.

2. Preliminary Considerations

2.1. Laser Heating. The temperature change after a laser pulse, assuming a negligible penetration depth of the light (i.e., that all the nonreflected part of the radiation is instantaneously converted into heat at the surface of the electrode), is given by the following expression:[22]

$$\Delta T(t) = \frac{1}{\sqrt{\pi\kappa c d} + \sqrt{\pi\kappa_1 c_1 d_1}} \int_0^t q(t-t') \frac{1}{\sqrt{t'}} \mathrm{d}t' \quad (1)$$

where κ, c, and d and κ_1, c_1, and d_1 are the thermal conductivity, thermal capacity, and density of the metal and the aqueous solution, respectively. q is the power density adsorbed by the metal, which depends on the temporal shape of the laser pulse:

$$q(t) = (1-R)I(t) \quad (2)$$

where R is the reflectivity of the surface and $I(t)$ is the time-dependent energy flux per unit of area.

For a uniform laser pulse the integration of eq 1 can be evaluated easily, resulting in the following:

$$\left[\Delta T(t) = \frac{2(1-R)I}{\sqrt{\pi\kappa c d} + \sqrt{\pi\kappa_1 c_1 d_1}} \sqrt{t} \quad t \le t_0 \quad \text{Heating}\right] \quad (3)$$

$$\left[\Delta T(t) = \frac{2(1-R)I}{\sqrt{\pi\kappa c d} + \sqrt{\pi\kappa_1 c_1 d_1}} [\sqrt{t} - \sqrt{t-t_0}] \quad t > t_0 \quad \text{Cooling}\right] \quad (4)$$

For long times, it is possible to expand the $\sqrt{t-t_0}$ term, keeping only the lower terms in the series. According to this approximation the temperature falls with time as

$$\Delta T(t) = \frac{1}{2}\Delta T_0 \sqrt{\frac{t_0}{t}} \quad (5)$$

and if the temperature change is small enough to allow a linear variation of the potential with the temperature, we can write

$$\Delta E = \left(\frac{\partial E}{\partial T}\right)_q \Delta T = \left(\frac{\partial E}{\partial T}\right)_q \frac{1}{2}\Delta T_0 \sqrt{\frac{t_0}{t}} \quad (6)$$

Then, the temperature coefficient of the open circuit potential can be extracted from the slope of the plot of ΔE vs $1/\sqrt{t}$. Moreover, from the electrocapillary equation it is possible to show[6,8]

$$\left(\frac{\partial E}{\partial T}\right)_q = -\left(\frac{\partial \Delta S}{\partial q}\right)_T \quad (7)$$

where ΔS is the interfacial entropy of formation of the interface. Hence, by integrating a plot of the slopes of the ΔE vs $1/\sqrt{t}$ as a function of the double-layer charge, it is possible to obtain a plot of ΔS. Note that when the curve ΔS vs q passes through a maximum, $(\partial \Delta S/\partial q)_T$ will be zero, and so will be the potential change due to the electrode heating. Hence, the potential of zero transient (pzt) can be identified with the potential of maximum entropy of double-layer formation.

TABLE 1: Thermodynamic Data for Hydrogen upd on Pt(111)[24]

	ΔH_{ads}/ kJ mol^{-1}	ΔS_{ads}/ J mol^{-1} K^{-1}	ΔG_{ads}/ kJ mol^{-1}	ω/ kJ mol^{-1}	K_{eq}/ dm^3 mol^{-1}
isothermal	−45	−65	−26	27	3.12×10^4
nonisothermal	−20.1	18.6			

2.2. Effect of the Adsorption Kinetics. Equation 6 is only valid when the change of interfacial potential is proportional to the change of the temperature. This behavior has been observed for purely capacitative behavior on Au(111) electrodes.[2] However, when specific adsorption takes place, finite relaxation times are observed.[2] For Pt(111), kinetics of hydrogen and anion adsorption are expected to affect the response after the laser-induced temperature change.

The thermodynamics of hydrogen adsorption on Pt(111) has been investigated by studying the influence of the temperature on the cyclic voltammogram, and from that, on the hydrogen isotherm. A Frumkin isotherm has been proposed with a strong repulsive interaction parameter.[23−25] In ref 24 a generalized isotherm was proposed. However, the plots of ΔG vs coverage are nearly straight lines, suggesting that the use of the Frumkin isotherm is justified. Jerkiewicz et al.[24] published values of the different thermodynamic functions for hydrogen adsorption on Pt(111), i.e., ΔG_{ads}, ΔH_{ads}, and $\Delta S_{ads.}$ The values of these thermodynamic magnitudes at zero coverage, together with the interaction parameter, ω, are given in Table 1.[26] The kinetics of hydrogen adsorption can be approximated accordingly:[28]

$$\frac{\mathrm{d}\theta}{\mathrm{d}t} = k_f(1-\theta)c_{H^+} \exp\left[-0.5\frac{F}{RT}E - 0.5g\theta\right] - k_b\theta \exp\left[0.5\frac{F}{RT}E + 0.5g\theta\right] \quad (8)$$

where θ is the fractional surface coverage and k_f and k_b are the forward and backward rate constants for the chemical reaction

$$\mathrm{Pt} + \mathrm{H}^+ + \mathrm{e} \underset{k_b}{\overset{k_f}{\rightleftharpoons}} \mathrm{Pt{-}H} \quad (9)$$

and g is the dimensionless interaction parameter ($g = \omega/RT$, where ω given in Table 1), which takes into account the increase in the activation energy for the adsorption as the coverage increase, as a consequence of lateral interactions.

For equilibrium $\mathrm{d}\theta/\mathrm{d}t = 0$ and eq 8 reduces to the Frumkin adsorption isotherm:

$$\frac{\theta}{1-\theta} = K_{eq} c_{H^+} \exp\left[-\frac{F}{RT}E - g\theta\right] \quad (10)$$

where $K_{eq} = k_f/k_b$; when the interaction parameter is close to zero, eq 10 reduces to the Langmuir isotherm. K_{eq} is related with the Gibbs energy of adsorption by

$$K_{eq} = \exp\left[-\frac{\Delta G_{ads}}{RT}\right] = \exp\left[-\frac{\Delta H_{ads}}{RT} + \frac{\Delta S_{ads}}{R}\right] \quad (11)$$

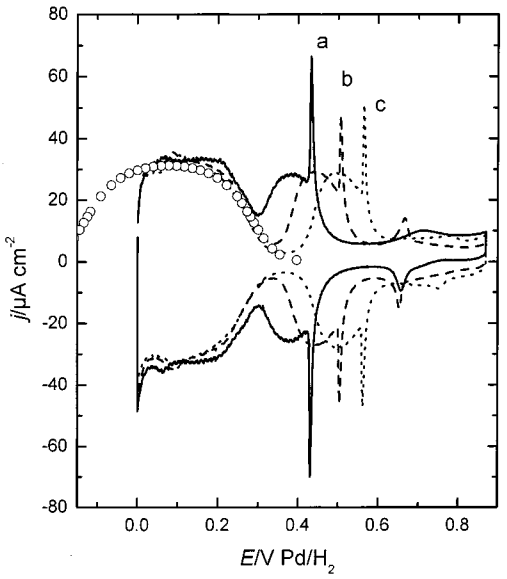

Figure 1. Cyclic voltammograms corresponding to a Pt(111) electrode in (a) 0.1 M H_2SO_4; (b) 0.1 M K_2SO_4 + 0.01 M H_2SO_4; (c) 0.1 M K_2SO_4 + 0.001 M H_2SO_4. Sweep rate: 50 mV s^{-1}. Open circles correspond to the current density calculated from the Frumkin isotherm, eq 12.

From eq 10 the adsorption pseudocapacitance can be obtained as a parametric function of the potential,

$$C = \frac{q_{ML}}{(\partial E/\partial\theta)} = -q_{ML}\frac{F}{RT}\frac{\theta(1-\theta)}{K_{eq} + g\theta(1-\theta)}$$

$$E = \frac{-RT}{F}\ln\frac{\theta}{K_{eq}c_{H^+}(1-\theta)} - \frac{RT}{F}g\theta \qquad (12)$$

where q_{ML} is the charge corresponding to the formation of a monolayer of hydrogen on Pt(111) (241 μC cm^{-2}). The resulting curve is with the experimental voltammograms in Figure 1.

It is useful to define an exchange current density[29] corresponding to the equilibrium condition $d\theta/dt = 0$:

$$j_0 = q_{ML}k_f(1-\theta_r)c_{H^+}\exp\left[-0.5\frac{F}{RT}E_r - 0.5g\theta_r\right] = q_{ML}k_b\theta_r\exp\left[0.5\frac{F}{RT}E_r + 0.5g\theta_r\right] \qquad (13)$$

To take into account the dependence of the rate constants with the temperature, we can write

$$k_f = k_f'\exp\left[-\frac{\Delta H_f^{\#}}{RT}\right] \quad \text{and} \quad k_b = k_b'\exp\left[-\frac{\Delta H_b^{\#}}{RT}\right] \qquad (14)$$

According to eq 11, k_f° and k_b° and $\Delta H_f^{\#}$ and $\Delta H_b^{\#}$ are related by

$$\frac{k_f'}{k_b'} = \exp\left[\frac{\Delta S_{ads}}{R}\right] \quad \text{and} \quad \Delta H_{ads} = \Delta H_1^{\#} - \Delta H_2^{\#} \qquad (15)$$

The response after the laser-induced temperature change will be due both to the double-layer contribution and that due to the electron-transfer reaction due to the modification of the hydrogen adsorption equilibrium.

$$\Delta E(t,\theta) = b_{dl}\Delta T + \frac{q_{ML}}{C_{dl}}\Delta\theta \qquad (16)$$

where C_{dl} is the double-layer capacity, ca. 20 μF cm^{-2},[19] and b_{dl} stands for the response of the double-layer potential to the increase of the temperature. The positive sign for the second contribution in the right-hand side of eq 16 reflects the fact that adsorption of hydrogen withdraws electrons, making the potential increase.

Equations 8 can be solved in combination with (3), (4), and (16) in order to explore the effect of different parameters on the laser-induced response.

3. Experimental Section

The experimental protocol has been described elsewhere.[2] Briefly, after recording a voltammogram to ensure the surface order and cleanliness of the solution, the electrode is polarized at a given potential. Around 200 μs before firing the laser, the counter electrode is disconnected and the potential of the working electrode is measured while the laser is fired at the surface, producing the rise of the temperature. The experiment was repeated at a frequency of 10 Hz, which allows the attainment of the equilibrium temperature between consecutive pulses. The counter electrode is reconnected between successive laser pulses, ensuring that the potential is kept at the desired value. A total of 256 potential transients were averaged at each potential using a TDS 3032 Tektronix oscilloscope. The light source employed was a GCR 130 Q-switched Nd:YAG laser (Spectra Physics Lasers, Inc.) operating in frequency-doubled mode at a wavelength of 532 nm and pulse duration of 10 ns. The beam diameter obtained directly at the laser output is ca. 7 mm and this was reduced to ca. 4 mm by passing it through a conventional arrangement of lenses. Optics housings and lenses were supplied by the Newport Corp. and mirrors obtained from Comar Instruments (Cambridge, U.K.). The laser power was determined with a Gentec ED-200LA detector head in conjunction with a Gentec SUN Series EM-1 Energy Meter. A laser energy of ca. 1−5 mJ per pulse, i.e., 14−70 mJ cm^{-2}, was used, well below the damage threshold of the electrode.

Experiments were performed in a conventional three-electrode arrangement. The Pt(111) single-crystal electrode was prepared at the University of Alicante from a small platinum bead (2 mm), oriented, cut and polished to obtain the Pt(111) orientation, following Clavilier's procedure.[30] Prior to each experiment the electrode was flame annealed in a butane + air flame, cooled in the atmosphere of the laboratory and then protected with a drop of ultrapure water. A platinum mesh (Goodfellow Cambridge Ltd., Cambridge, U.K.) was used as a counter electrode and a Pd wire charged with H_2 in a separate compartment was used as a reference electrode. Cyclic voltammograms were recorded using a computer-controlled μ-Autolab potentiostat (Eco-Chemie, Utrecht, Netherlands) with the current integration mode.

Solutions were prepared from concentrated sulfuric and perchloric acids (Fisher Scientific, for Trace Metal Analysis), K_2SO_4 (SIGMA, SigmaUltra) and $KClO_4$ (Aldrich, ACS reagent) diluted in ultrapure water (resistivity not less than 18 MΩ cm) obtained from a Elgastat water purification system (USF Ltd., Bucks., U.K.). $KClO_4$ was purified by recrystallization. The other chemicals were used as received, without further purification.

4. Computational Details

Solution of the differential equation resulting from eqs 8−16 has been done by using a fifth-order Runge−Kutta method with adaptive step size routine written in Fortran77.[31]

To take into account the depletion of protons in the diffusion layer due to its consumption during the hydrogen adsorption

process, we solved the diffusion equation:

$$\left(\frac{\partial c_{H^+}}{\partial t}\right) = D\left(\frac{\partial^2 c_{H^+}}{\partial x^2}\right) \quad (17)$$

where D is the diffusion coefficient for the protons,[32] 9.31×10^{-5} cm^2 s^{-1}, considered as constant. Equation 17 is subjected to the following boundary condition:

$$c(t, x \rightarrow \infty) = c_{bulk}$$
$$c(t=0, x) = c_{bulk} \quad (18)$$

together with the corresponding Neumann condition at the surface of the electrode for the flux of protons derived for eqs 8−16. The solution was computed with a fully implicit algorithm written in Fortran77.

5. Results

Figure 1 shows cyclic voltammograms corresponding to a Pt(111) single-crystal electrode in sulfuric acid + potassium sulfate solutions of different pHs. These voltammograms are well-known in the literature[33−35] and only the main features will be described here. Two regions can be clearly distinguished. The region located at lower potentials corresponds to hydrogen adsorption. Only two-thirds of a monolayer (160 μC cm^{-2}) is attained before the hydrogen evolution reaction starts. This region remains almost unaffected by an increase of the pH. The region located at potentials higher than 0.35 V corresponds to anion adsorption. The shift of the anion adsorption region with the pH reflects the displacement of the Pd/H_2 reference potential, which follows the reversible hydrogen adsorption. The sharp spike at the end of the anion adsorption region has been assigned to a disorder/order phase transition. An ordered $(\sqrt{3}\times\sqrt{7})$R19° has been observed in situ with STM at potentials positive to this spike.[36]

Also in Figure 1 is shown the current density expected from the pseudocapacity calculated with the Frumkin isotherm (eq 10), using the values of g and ΔG_{ads} shown in Table 1. The potential has been adapted from the SCE to the Pd/H_2 reference electrode by subtracting 50 mV.[37] The reasonable agreement between experimental and calculated curves supports the use of eqs 8−16 to explain the potential transients obtained after the laser illumination.

Figure 2 shows potential transients obtained after laser illumination of the Pt(111) electrode surface. For clarity, they have been plotted in two different graphs, Figure 2A showing the transients obtained in the hydrogen adsorption region and Figure 2B showing those corresponding to the sulfate adsorption region. The cyclic voltammogram in the inset has been included for the sake of clarity. In it, the vertical dotted lines mark the potentials at which the laser-induced transients have been recorded. The transients in the hydrogen adsorption region show a bipolar shape, with a sharp negative peak at shorter times, and a broader positive peak after that. At longer times, the potential shift becomes negative again and does not recover its initial value, at least in the time window of the experiment. Inspection of Figure 2B shows that the transients change sign when the potential is moved into the anion adsorption region (between 0.3 and 0.4 V), becoming positive at 0.4 V. Finally, another change of sign occurs after the spike corresponding to the formation of the $(\sqrt{3}\times\sqrt{7})$ ordered adlayer, the transients being negative in the higher potential region. The potential transient recorded just after the spike at 0.5 V is positive;

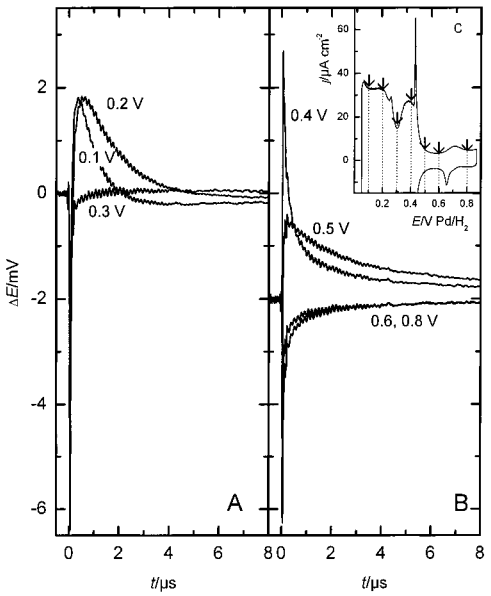

Figure 2. Laser-induced potential transient for the Pt(111) electrode in 0.1 M H_2SO_4 at different potentials: (A) 0.1−0.3 V and (B) 0.4−0.8 V, as labeled. Inset (C): Relative position to the CV of the potentials corresponding to the laser-induced transients in A and B. Laser energy: 2 mJ/pulse.

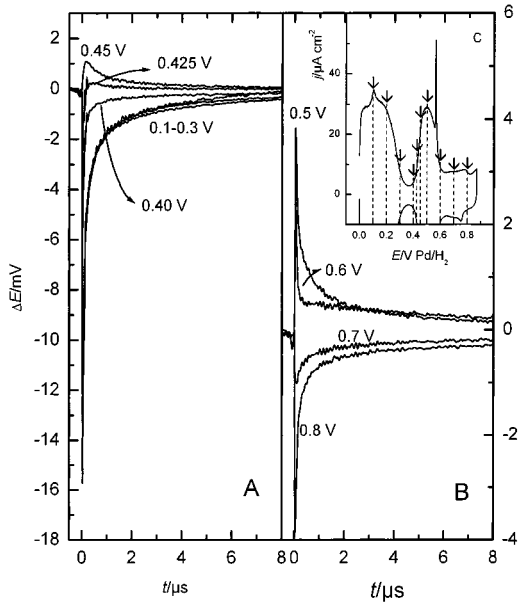

Figure 3. As Figure 2 but for a 0.1 M K_2SO_4 + 0.001 M H_2SO_4 solution. Laser energy: 1 mJ/pulse.

however, careful inspection of the latter shows a negative peak at very short times. Potential transients of similar shape have been reported for Au(111) in the same solution, also in the potential region corresponding to sulfate adsorption.[2] They have been explained as a consequence of the overlapping of two processes with different relaxation times. The process at shorter times was identified with the thermodiffusion potential established as a consequence of the temperature gradient existing in the solution between the working and the reference electrodes. This potential was estimated negative from the entropies of transport of the ions present in solution, in agreement with the sign observed in the transient at short times. Similar interpretation seems valid in the present case.

Figure 3 shows the laser-induced potential transients obtained at similar potentials, but in a solution of higher pH: 0.1 M K_2SO_4 + 1 mM H_2SO_4. As in Figure 2, Figure 3A shows the

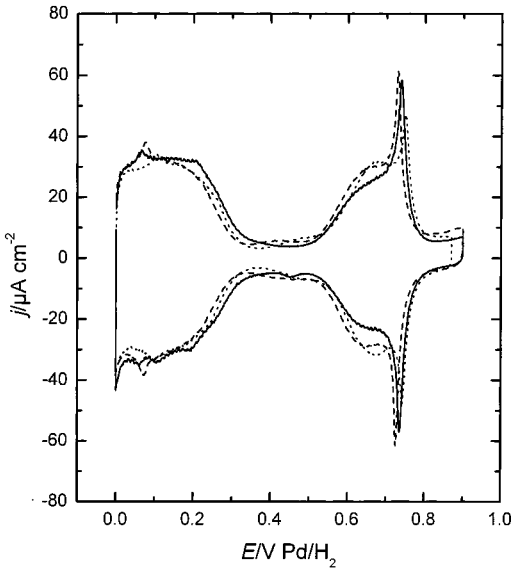

Figure 4. Cyclic voltammograms corresponding to a Pt(111) electrode in 0.1 M $HClO_4$ (solid line), 0.1 M $KClO_4$ + 0.01 M $HClO_4$ (dashed line), and 0.1 M $KClO_4$ + 0.001 M $HClO_4$ (dotted line). Sweep rate: 50 mV s^{-1}.

laser-induced potential transients in the hydrogen adsorption region and Figure 3B those obtained in the sulfate adsorption region. Observation of Figure 3A shows that the bipolar shape observed in the hydrogen adsorption region at lower pH is not observed. The potential transients are now negative between 0.1 and 0.4 V, decreasing in magnitude as the potential is increased in this region. In contrast, in the higher potential region, Figure 3B shows behavior similar to that in Figure 2B. The transients are positive in the beginning of the sulfate adsorption region and become negative when the potential is increased beyond the sharp spike at 0.57 V. An important difference in the transients in this potential region is observed when the transient at 0.5 V in Figure 2B is compared with that obtained at 0.6 V in Figure 3B. They both correspond to the same relative position in the sulfate adsorption wave: just after the sharp spike. A negative contribution is observed in the first one at short times, as discussed in the previous paragraph. A fast contribution at short times is also observed in the transient at 0.6 V in the higher pH, but now with positive sign. The same change of sign was observed, as reported previously,[2] on Au(111) in the same solutions, and shown to be correlated with the expected change of sign for the thermodiffusion potential predicted from the entropy of transport of the ions present in both solutions.

Figure 4 shows cyclic voltammograms corresponding to the Pt(111) electrode in perchloric acid and potassium perchlorate solutions. These voltammograms are similar to those reported in the literature for the same conditions.[10,38] Comparison of Figures 1 and 4 shows that, while the hydrogen adsorption region remains almost unaltered after the change of the electrolyte, the region attributed to the sulfate adsorption in the voltammograms of Figure 1 has disappeared and a new adsorption region is observed at higher potentials, between 0.5 and 0.85 V. This latter adsorption region is usually attributed to adsorption of oxygenated species,[39,40] namely hydroxyl adsorption. The invariance of its position when the pH is changed (against a reference electrode following the RHE) support this hypothesis.[33]

The laser-induced potential transients obtained in 0.1 M $HClO_4$ are shown in Figure 5. The potential transients obtained in the hydrogen adsorption region are similar to those obtained in 0.1 M H_2SO_4 and show again the bipolar shape, with a fast negative response at shorter time, a broader positive peak and a second change in sign, reaching an almost constant negative value at longer times. The potential transients change sign between 0.3 and 0.4 V, being positive at the higher potentials. While the behavior in the hydrogen adsorption region is similar to that observed in sulfuric acid solutions, different behavior is observed at higher potentials: the intensity of the transients is a maximum around 0.5 V and decreases in magnitude when the potential is further increased into the region of adsorption of oxygenated species. Finally, the transients become negative well after the spike, at potentials higher than 0.9 V.

As happened with the potential transients obtained in sulfuric solutions of higher pH, those obtained in a 0.1 M $KClO_4$ + 1 mM $HClO_4$ (Figure 6) do not exhibit the bipolar shape in the hydrogen adsorption region. As before, the potential transients change sign between 0.4 and 0.5 V, becoming positive at potentials higher than 0.45 V.

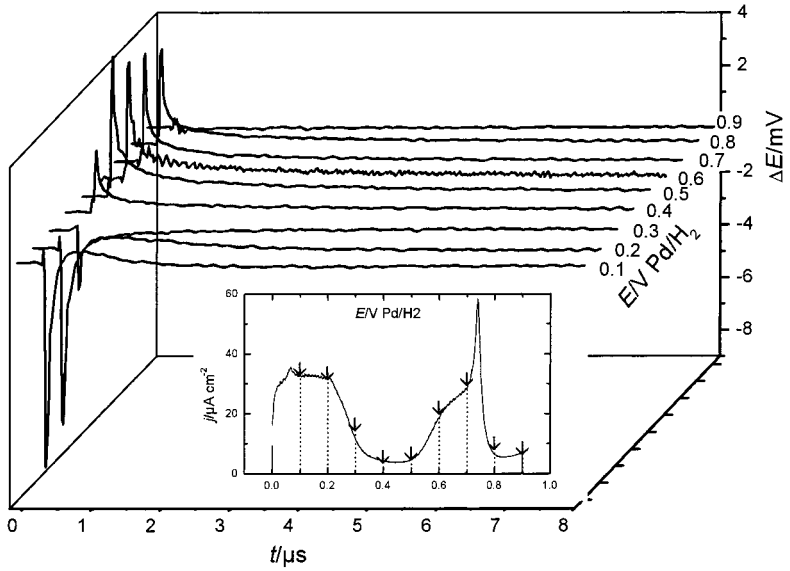

Figure 5. As Figure 2 but for a 0.1 M $HClO_4$ solution. Laser energy: 1 mJ/pulse.

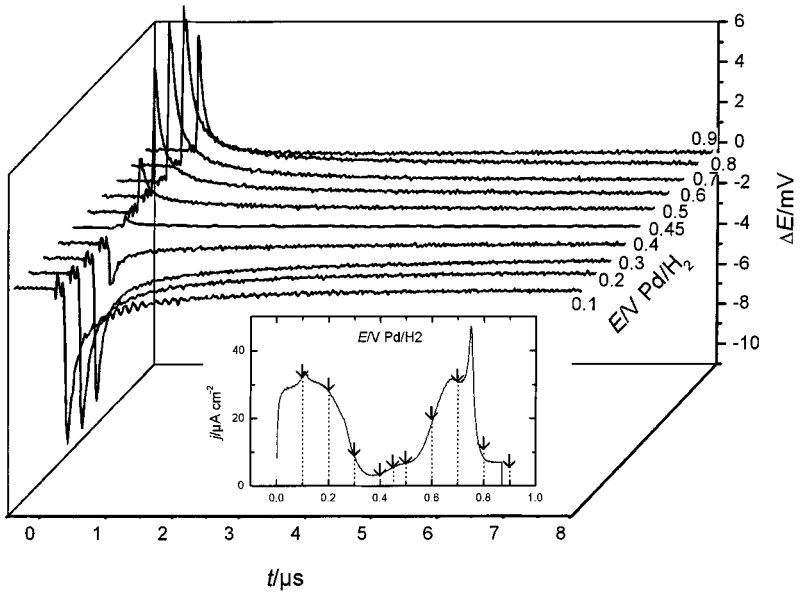

Figure 6. As Figure 2 but for a 0.1 M $KClO_4$ + 0.001 M $HClO_4$ solution. Laser energy: 1 mJ/pulse.

6. Discussion

We have shown in a previous publication that by measuring laser-induced potential transients and the use of eq 7 it is possible to get a plot of relative values of the entropy of formation of the double layer.[2] We applied this methodology to the case of Au(111) in perchloric and sulfuric acid solutions. In that case, approximate parabolic plots were obtained for the entropy of formation of the double layer with the potential of the maximum located at a potential slightly negative to the pzc. This is in agreement with models of the double layer and indicates that water molecules are adsorbed to the metal surface at the pzc through the oxygen, in such a way that a slightly negative charge on the metal is necessary to attain a maximum degree of looseness of the water molecules at the interface.[6−8] Then, the positive thermal coefficient at the pzc can be interpreted as a consequence of the negative contribution of the water dipoles to the potential drop at the metal|solution interface at this potential.

The application of the previous interpretations to the present system is complicated by the existence of charge-transfer processes. It is clear from the potential transients in Figures 2 and 5 that the potential does not follow the temperature change in the hydrogen adsorption region. To take into account the kinetic of hydrogen adsorption, we need to use eqs 8−16. Figure 7 shows potential transients simulated with these equations, for different values of the rate constant, k_f, at 0.1 V (vs Pd/H_2). To do this simulation, we have selected values for the thermal coefficient of the double-layer potential, b_{dl}, and the activation energy, $\Delta H_f^{\#}$ which give a reasonable agreement with the experimental behavior (see below). The corresponding changes in the hydrogen coverage due to the change of the potential are plotted in Figure 7 (inset). Two extreme behaviors are observed for relatively high or low values of the time constant. If the time constant is low enough, there is not enough time for the charge-transfer process and the hydrogen coverage remains unaltered during the potential transient. In this case, the potential follows the shape of the temperature change. On the other hand, when the rate constant is high enough, the hydrogen adsorption can be considered as at equilibrium at each instant, and both the hydrogen coverage and the potential transient follow the change of the temperature. In this case, the change of the potential is smaller, since it is buffered by the hydrogen

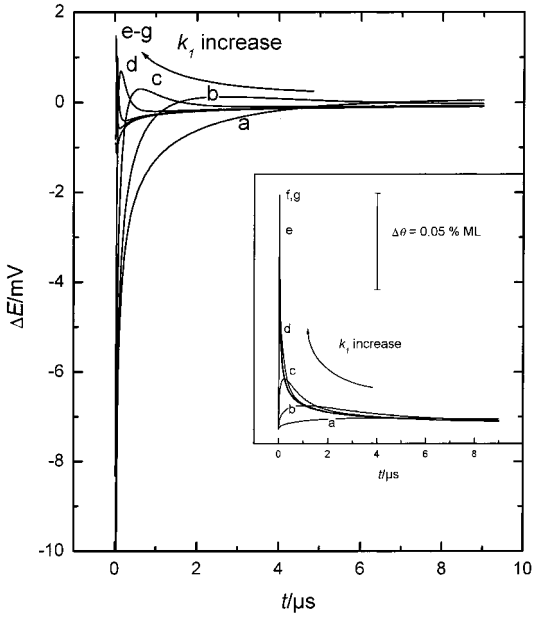

Figure 7. Simulated potential transients for different values of the rate constant k_1: $\log(k_1/M^{-1}\,s^{-1})$ = (a) 5.6, (b) 6.2, (c) 6.8, (d) 7.4, (e) 8.0, (f) 8.3, (g) 8.9. Laser energy: 1 mJ/pulse; $b_{dl} = -3$ mV K^{-1}. Inset: Change of the hydrogen coverage during the potential transient.

adsorption reaction. For intermediate values of the rate constant potential transients similar to those shown in Figures 2A and 5, corresponding to sulfuric and perchloric acid solutions, are obtained. The particular shape of these transients can be understood as follows: at the beginning of the transient, the sudden increase of the electrode temperature would cause a decrease of the electrode potential as a consequence of the negative thermal coefficient of the double layer (b_{dl}). Negative values of b_{dl} are expected for potentials negative to the pzc.[2] The decrease of the electrode potential would cause an increase of the hydrogen coverage. However, the hydrogen adsorption reaction would withdraw electrons from the electrode, tending to increase its potential. As a consequence of these opposing effects, double-layer and charge-transfer processes, the potential transient exhibit a bipolar shape.

When the pH is increased, the rate of the hydrogen adsorption process is slowed, according to eq 8. Figure 8A shows the

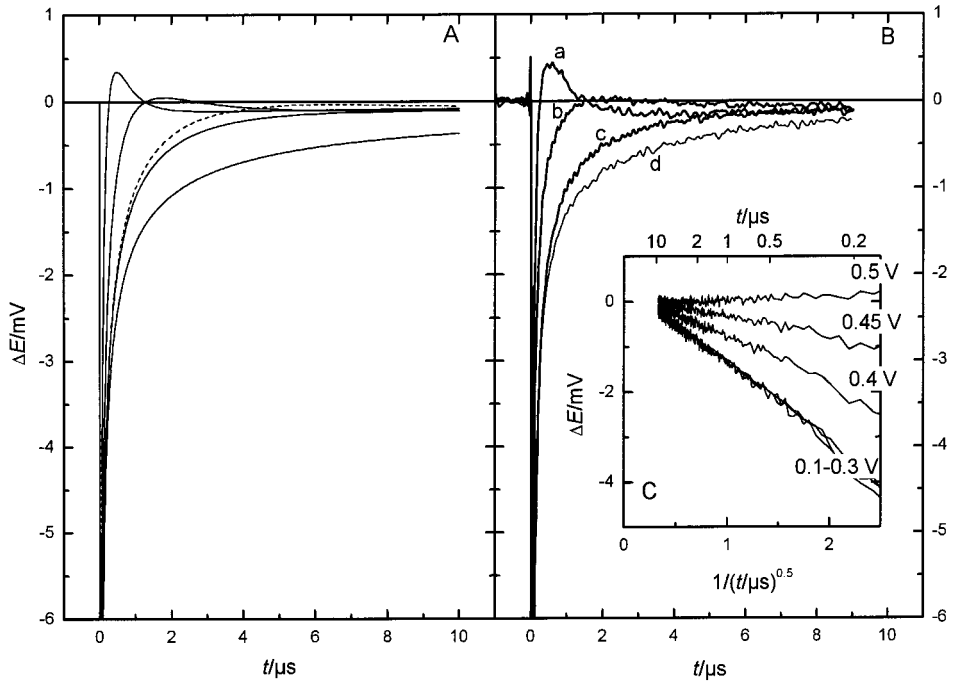

Figure 8. Comparison of simulated (A) and experimental (B) potential transients after laser illumination. (A) Simulated curves: $b_{dl} = -3$ mV K^{-1}, $\log(k_1/\mathrm{M}^{-1}\ \mathrm{s}^{-1}) = 6.9$, $\Delta H_1^{\#} = 40$ kJ mol^{-1}; dashed line corresponds to simulation without considering depletion of proton on the diffusion layer. (B) Experimental curves for x M $KClO_4$ + y M $HClO_4$ solutions: (a) $x = 0$, $y = 0.1$; (b)−(d) $x = 0.1$ and $y = 0.01$, 0.001, and 10^{-4}, respectively. Laser energy = 1 mJ/pulse. (C) plot of the potential transients, between 0.1 and 0.5 V as labeled, in 0.1 M $KClO_4$ + 10^{-4} M $HClO_4$, as a function of the reciprocal of the square root of time.

simulated behavior for higher pHs at 0.1 V (vs Pd/H_2), while Figure 8B shows the experimental results. To obtain the better agreement between experimental and simulated transients, the potential transient at pH ≈ 4 (0.1 M $KClO_4$ + 0.1 mM $HClO_4$) was used to estimate the value of the thermal coefficient of the double layer, b_{dl}. At this low concentration of protons the rate of hydrogen adsorption is so slow that it is not able to follow the temperature change; the hydrogen coverage can be considered as frozen during the potential transient. This conclusion is extracted from the plot of the potential transient as a function of the reciprocal of the square root of time, shown in Figure 8C whose linearity is in agreement with eq 6. By using this value of b_{dl}, the rate constant was varied to find the best fit between the experimental and simulated curves. This was observed for a value of k_1 ca. 8×10^6 mol^{-1} dm^3 s^{-1}. The activation energy ($\Delta H_1^{\#}$) has little effect in the simulated curves, being very difficult to get a reliable estimation of this parameter. The value for the rate constant should be compared with those reported by means of electrochemical impedance spectroscopy.[20,21] Our value of rate constant is equivalent to an exchange current density, according to eq 13, of $j_0 = 0.5$ A cm^{-2}, from which a value of the equivalent resistance to the charge transfer can be calculated according to

$$R_{ct} = \frac{RT}{Fj_0}; \qquad 0.045\ \Omega\mathrm{cm}^2 \tag{19}$$

Values of charge-transfer resistance for hydrogen underpotential deposition (upd) on polycrystalline platinum are around[20] 0.06 Ω cm^2; higher values have been reported for Pt(100) and Pt(311), namely 0.37 and 0.09 Ω cm^2, respectively.[20] The rate of hydrogen adsorption on Pt(111) has been recently measured by impedance methods and a value of ca. 0.03 Ω cm^2 has been reported.[21] Those values are in reasonably good agreement with our estimated result, giving support to our interpretation of the potential transient induced by laser irradiation.

It is worth pointing out that, although the value of b_{dl} is affected by the uncertainty in the estimation of the maximum change of the electrode temperature from eq 3, mainly coming from the knowledge of the surface reflectivity and the inaccuracy in the positioning of the electrode, this uncertainty is not reflected in the estimation of the rate constant: different fittings of the experimental data for different values of ΔT_0 lead always to almost identical values of k_1.

The four solid curves in Figure 8A have been obtained with identical values of b_{dl}, k_1, and $\Delta H_f^{\#}$, only changing the concentration of protons in the solution. While mass transport limitations exert very little effect for the 0.1 M solution, for the higher pHs they become significant. As an example, the dotted line was obtained by neglecting the consumption of protons in the solution of pH ≈ 3 (0.1 $KClO_4$ + 1 mM $HClO_4$). From the observation of the transients of Figure 8A we conclude that the limitations imposed to the hydrogen adsorption process when the proton concentration is decreased result in a potential transient that reflects mainly the response of the double layer to the temperature change.

If we accept that the potential transients in Figures 3A and 6 reflect mainly the response of the double-layer potential to the increase of the temperature, then the potential of zero response observed between 0.4 and 0.45 V (vs Pd/H_2) in those figures would correspond, according to eq 7, to the pme.

The temperature coefficient of the metal|solution potential drop can be split into three contributions:[41]

$$\left(\frac{\partial \phi^{\mathrm{M-S}}}{\partial T}\right)_{\sigma,m} = \frac{1}{e}\left(\frac{\partial \Phi}{\partial T}\right)_{\sigma} + \left(\frac{\partial \phi^2}{\partial T}\right)_{\sigma,m} + \left(\frac{\partial \phi^{\mathrm{w}}}{\partial T}\right)_{\sigma,m}$$

where Φ is the work function at the given charge σ, ϕ^2 is the potential drop at the diffuse layer, and ϕ^{w} is contribution to the potential drop due to solvent structuring. The contribution due to the thermal coefficient of the potential drop through the diffuse layer can be estimated by the Gouy−Chapman theory

and shown, for the electrolyte concentration employed in the present study, to be relatively very small (0.15 mV K^{-1} at 20 μC cm^{-2} for a uni-univalent electrolyte). The temperature coefficient of the work function can only be measured directly at $\sigma = 0$. For Pt(111) the thermal coefficient of the work function has been measured,[42] amounting to $\Delta\Phi/\Delta T = -1.5 \times 10^{-4}$ eV K^{-1}. Although this value is only valid for zero charge, it is useful to give an idea of the order of magnitude expected for this contribution. This figure is small in comparison with the values of the potential transients obtained and can be neglected in an approximate discussion of the trends observed in Figures 3 and 6. Then, the potential transients are mainly determined by the effect of the temperature on the structure of the solvent dipoles in the interphase. Similarly, it has been previously concluded that the salient features of the entropy of formation of the double layer reflects mainly the contribution from the rearrangement of interfacial water.[5,9]

Hence, the change of sign of the potential transient after the increase of the temperature can be understood as a change of the sign of the dipolar contribution to the potential drop, which would decrease as a consequence of the disorder induced by the increase of the temperature. The negative transients at lower potentials can then be explained as a decrease of a positive contribution from the layer of water dipoles. On the other hand, the positive transients at higher potentials would reflect a decrease in the absolute value of a negative contribution to the potential drop. The change in the sign of the dipolar contribution is expected to take place at the pme, since at this potential the dipolar contribution is minimum. Moreover, the pme is expected to be located in the vicinity of the pzc. This has been shown to be the case for mercury[6−8] and single-crystal gold[2−5] electrodes. Then, if the correlation between the pme and the pzc[43] is maintained in the case of Pt(111), we would locate the pzc for this electrode surface around 0.45 V. The preceding discussion neglects, however, the natural orientation of water molecules by its chemical interaction with the metallic surface. This chemical interaction is responsible for a small shift of the pme with respect to the pzc in the case of gold single crystals.[3−5]

As stated in the Introduction, the measurement of the pzc for platinum electrodes has hitherto been precluded due to the existence of the hydrogen and anion adsorption reactions. These not only introduce experimental difficulties to its determination but also conceptual ambiguity. Due to the existence of a charge transfer process, the interface cannot be considered ideally polarizable and the introduction of the thermodynamic concept of total charge becomes necessary. The total charge is the quantity measurable thermodynamically, but on account of the charge-transfer process it may not be equal to the actual free charge on the metal.[44,45]

Different methods have been applied in the past for the determination of the pzc of Pt(111) in perchloric acid solutions, based on indirect observations: CO charge displacement,[14] N_2O reduction,[13] immersion methods,[12] IR observation[46] and electrochemical impedance measurements.[19] We should bear in mind that, while the first three methods are sensitive to the total charge on the electrode, the latter two are presumably sensitive to the free charge. Apart from the immersion method, which gave a value for the pztc at 0.84 V (RHE), i.e., into the hydroxide adlayer region, the other results agree in locating the pztc at the onset of hydrogen adsorption (i.e., 0.34 V RHE[14,39]) or within the double-layer region.[13,19] From the location of the pztc in the hydrogen region it would conclude that the pzfc must be located at lower potentials, and an estimation of it can be done by considering a constant value for the double-layer capacity.[14] However, as shown later,[18] this estimation needs to consider the remaining charge in the double layer after the CO displacement. This correction shifts both the pztc and the pzfc toward more positive values. While the correction is small for the pztc, due to the relatively large value of the pseudocapacity, it is significant for the pzfc. The influence of the pH on the location of the pztc of Pt(111) electrodes has also been studied by the CO charge displacement method.[14] The pztc was found to be independent of the pH in the RHE scale (shifts ca. 60 mV/decade in a pH independent scale), being located at the onset of hydrogen adsorption.

The change of sign in the potential transient shown in Figures 3 and 6 between 0.4 and 0.45 V suggests that the pzfc lies in the double-layer region, according to the discussion above, for solutions of pH 3. This value would be higher than that predicted by the CO charge displacement.[14] However, we should bear in mind that both estimations either rely on indirect observation or need unavailable corrections. In this regard the residual charge on the CO adlayer after the charge displacement could be responsible for shifting the estimated pztc from the double-layer region into the hydrogen region. In this case a significant amount of charge (ca. 18 μC cm^{-2}) would be necessary on the CO-saturated metal|solution double layer in order to produce this shift, which seems in contradiction with the very small double-layer capacitance observed for the CO covered electrode. While a very high value of pzc for the CO saturated surface has been estimated from work function measurements in UHV,[18] namely 1.0 ± 0.2 V (vs SHE), there is no direct measurement of this parameter in the electrochemical environment, which would be needed to further test this point. In this respect, preliminary measurements of the laser-induced potential transients on the CO covered electrode are consistent with a negatively charged electrode over the whole potential range of stability of the CO adlayer. Besides, if the pzc of the CO saturated double layer remains constant (in a pH independent reference scale), the residual charge after the CO displacement would be higher as the pH is increased. However, it is still difficult to conclude if this effect could explain the discrepancies and more work would be necessary in order to completely solve the question.

In the preceding analysis we have not considered the effect of the thermoelectric potential. This potential would arise due to the difference in the temperature of the solutions at the working and reference electrodes.[47] This effect is more important in acid solutions due to the unusually large entropy of transport of the protons. However, it becomes less significant at higher pHs and its consideration would change the location of the pme very little. It is possible to estimate the thermodiffusion potential from the published values of the entropies of transport of the different ions present in the working solution. It can be shown that, for mixtures of $KClO_4$ + $HClO_4$ the thermodiffusion potential represents a small negative contribution, which would slightly displace the pme in the negative direction. However, this correction is expected to be small from the comparison of the potential of zero transient at different pHs.[2]

Another effect that deserves a comment is the influence of the pH on the location of the potential of zero transient. It is difficult to extract any conclusion in this respect from the experiments in the presence of sulfates, due to the overlapping of the anion adsorption region. However, some effect seem to be observed when Figures 5 and 6 are compared: while the potential transient at 0.4 V is clearly positive in 0.1 M $HClO_4$ solution, the transient at the same potential is still negative in the solution of pH = 3. This trend is confirmed by the experiments in the 0.1 M $KClO_4$ + 0.1 mM $HClO_4$ solution,

where the potential of zero transient is displaced to 0.49 V (see Figure 8C). It could be argued that there is a different contribution of the thermodiffusion potential in solutions of different pH, but this effect would tend to contribute negatively to the transient performed at the lower pH, i.e., in the opposite direction to the trend observed. Then it can be concluded that there is a positive shift (in the Pd/H_2 scale) of the potential of zero transient when the pH is increased that could just reflect its constancy in a pH independent reference scale.

We believe that the laser-induced potential transients presented in this work represent another piece of information into the controversial problem of the pzc of Pt(111) single-crystal electrodes. However, more work is still necessary to completely solve it.

Acknowledgment. V.C. gratefully acknowledges the European Commission for the award of a Marie Curie Fellowship under the European Community program "Improving Human Research Potential and the Socio-economic Knowledge Base" under contract number HPMFCT-2000-00529. The PTCL electronic workshop is gratefully acknowledged for the development of the potentiostat used in this work. We thank Prof. J. Feliu for generously loaning us the Pt(111) single-crystal electrode and B. Brookes for helpful assistance for the computer simulation of the diffusion problem.

References and Notes

(1) Climent, V.; Coles, B. A.; Compton, R. G. *J. Phys. Chem. B* **2001**, *105*, 10669−10673.

(2) Climent, V.; Coles, B. A.; Compton, R. G. *J. Phys. Chem. B* **2002**, *106*, 5258−5265.

(3) Hamelin, A.; Stoicoviciu, L.; Silva, F. *J. Electroanal. Chem.* **1987**, *229*, 107−124.

(4) Silva, F.; Sottomayor, M. J.; Hamelin, A. *J. Electroanal. Chem.* **1990**, *294*, 239−251.

(5) Silva, F.; Sottomayor, M. J.; Martins, A. *J. Chem. Soc., Faraday Trans.* **1996**, *92*, 3693−3699.

(6) Harrison, J. A.; Randles, J. E. B.; Schiffrin, D. J. *J. Electroanal. Chem.* **1973**, *48*, 359−381.

(7) Hills, G. J.; Hsieh, S. *J. Electroanal. Chem.* **1975**, *58*, 289−98.

(8) Silva, A. F. In *Trends in Interfacial Electrochemistry*; Silva, A. F., Ed.; ACS symposium series; D. Reidel Publishing Company: Amsterdam, 1986; pp 49−70.

(9) Aloisi, G.; Guidelli, R. *J. Electroanal. Chem.* **1989**, *260*, 259−267.

(10) Clavilier, J. *J. Electroanal. Chem.* **1980**, *107*, 211−216.

(11) Clavilier, J.; Faure, R.; Guinet, G.; Durand, R. *J. Electroanal. Chem.* **1980**, *107*, 205−209.

(12) Hamm, U. W.; Kramer, D.; Zhai, R. S.; Kolb, D. M. *J. Electroanal. Chem.* **1996**, *414*, 85−89.

(13) Attard, G. A.; Ahmadi, A. *J. Electroanal. Chem.* **1995**, *389*, 175−190.

(14) Climent, V.; Gómez, R.; Orts, J. M.; Aldaz, A.; Feliu, J. M. In *The Electrochemical Society Proceedings*; Korzeniewski, C., Conway, B. E., Eds.; The Electrochemical Society, Inc.: Pennington, NJ, 1997; Vol. 97-17, pp 222−237.

(15) Climent, V.; Gómez, R.; Feliu, J. M. *Electrochim. Acta* **1999**, *45*, 629−637.

(16) Climent, V.; Gómez, R.; Orts, J. M.; Aldaz, A.; Feliu, J. M. In *The Electrochemistry Society Proceedings*; Jerkiewicz, G., Feliu, J. M., Popov, B. N., Eds.; The Electrochemical Society, Inc.: Pennington, NJ, 2000; Vol. 2000-16, pp 12−30.

(17) Gómez, R.; Climent, V.; Feliu, J. M.; Weaver, M. J. *J. Phys. Chem. B* **2000**, *104*, 597−605.

(18) Weaver, M. J. *Langmuir* **1998**, *14*, 3932−3936.

(19) Pajkossy, T.; Kolb, D. M. *Electrochim. Acta* **2001**, *46*, 3063−3071.

(20) Morin, S.; Dumont, H.; Conway, B. E. *J. Electroanal. Chem.* **1996**, *412*, 39−52.

(21) Sibert, E.; Faure, R.; Durand, R. *J. Electroanal. Chem.* **2001**, *515*, 71−81.

(22) Benderskii, V. A.; Velichko, G. I. *J. Electroanal. Chem.* **1982**, *140*, 1−22.

(23) Markovic, N. M.; Grgur, B. N.; Ross, P. N. *J. Phys. Chem. B* **1997**, *101*, 5405−5413.

(24) Jerkiewicz, G. *Prog. Surf. Sci.* **1998**, *57*, 137−186.

(25) Zolfaghari, A.; Jerkiewicz, G. *J. Electroanal. Chem.* **1999**, *467*, 177−185.

(26) The values of the thermodynamic functions given in ref 24 are referred to a temperature variable standard state (isothermal cell). However, the laser-induced temperature change only affects the working electrode and leaves the reference electrode unaffected. Hence, the thermodynamic values need to be recalculated to the constant temperature reference state (nonisothermal cell), by taking into account the thermal coefficient of the standard hydrogen electrode (8.4×10^{-4} V K^{-1} [27]).

(27) Conway, B. E.; Angerstein-Kozlowska, H.; Sharp, W. B. *J. Chem. Soc., Faraday Trans. 1* **1978**, *74*, 1373−89.

(28) Angerstein-Kozlowska, H.; Klinger, J.; Conway, B. E. *J. Electroanal. Chem.* **1977**, *75*, 45−60.

(29) Angerstein-Kozlowska, H.; Conway, B. E. *J. Electroanal. Chem.* **1979**, *95*, 1−28.

(30) Clavilier, J.; Armand, D.; Sun, S.-G.; Petit, M. *J. Electroanal. Chem.* **1986**, *205*, 267−277.

(31) Press: W. H. *Numerical recipes in FORTRAN: the art of scientific computing*, 2nd ed.; Cambridge University Press: Cambridge, U.K., 1992.

(32) Lide, D. R.; Frederikse, H. P. R.; Chemical Rubber Company. *CRC handbook of chemistry and physics*, 79th ed.; CRC Press: Boca Raton, FL, and London, 1998.

(33) Al Jaaf-Golze, K.; Kolb, D. M.; Scherson, D. A. *J. Electroanal. Chem.* **1986**, *200*, 353−362.

(34) Wagner, F. T.; Ross, P. N. *J. Electroanal. Chem.* **1988**, *250*, 301−320.

(35) Feliu, J. M.; Orts, J. M.; Gómez, R.; Aldaz, A. *J. Electroanal. Chem.* **1994**, *372*, 265−268.

(36) Funtikov, A. M.; Stimming, U.; Vogel, R. *J. Electroanal. Chem.* **1997**, *428*, 147−153.

(37) Ives, D. J. G.; Janz, G. J. *Reference electrodes, theory and practice*; Academic Press: New York, 1961.

(38) Lazarescu, V.; Clavilier, J. *Electrochim. Acta* **1998**, *44*, 931−941.

(39) Clavilier, J.; Albalat, R.; Gómez, R.; Orts, J. M.; Feliu, J. M.; Aldaz, A. *J. Electroanal. Chem.* **1992**, *330*, 489−497.

(40) Herrero, E.; Feliu, J. M.; Wieckowski, A.; Clavilier, J. *Surf. Sci.* **1995**, *325*, 131−138.

(41) Guidelli, R.; Aloisi, G.; Leiva, E.; Schmickler, W. *J. Phys. Chem. B* **1988**, *92*, 6671−6675.

(42) Kaack, M.; Fick, D. *Surf. Sci.* **1995**, *342*, 111−118.

(43) If the pzc lies in the double-layer region, then pzfc and pztc become equal. We use the designation pzc in this case.

(44) Frumkin, A. N.; Petrii, O. A.; Damaskin, B. B. In *Comprehensive Treatise of Electrochemistry*; Bockris, J. O. M., Conway, B. E., Yeager, E., Eds.; Plenum: New York, 1980; Vol. 1, pp 221−289.

(45) Frumkin, A. N.; Petrii, O. A. *Electrochim. Acta* **1975**, *20*, 347−359.

(46) Iwasita, T.; Xia, X. H. *J. Electroanal. Chem.* **1996**, *411*, 95−102.

(47) Agar, J. N. In *Advances in Electrochemistry and Electrochemical Engineering*; Delahay, P., Tobias, C. W., Eds.; Wiley-Interscience: New York, 1963; Vol. 3, pp 31−121.